Life Sciences 317 (2023) 121464

Contents lists available at ScienceDirect

Life Sciences

journal homepage: www.elsevier.com/locate/lifescie

Adipocyte-hepatocyte crosstalk in cellular models of obesity: Role of soluble factors

Francesca Baldini [a,b], Farah Diab [b], Nadia Serale [c], Lama Zeaiter [a,b], Piero Portincasa [c], Alberto Diaspro [a,d,e], Laura Vergani [b,*]

[a] Nanoscopy, Istituto Italiano Tecnologia, Via Enrico Melen 83, 16152 Genova, Italy
[b] Department of Earth, Environment and Life Sciences (DISTAV), University of Genova, Corso Europa 26, 16132, Genova, Italy
[c] Clinica Medica "A. Murri", Department of Biomedical Sciences and Human Oncology, University of Bari, Medical School, Piazza Giulio Cesare 11, 70124 Bari, Italy
[d] Department of Physics (DIFILAB), University of Genoa, Via Dodecaneso 33, 16146 Genoa, Italy
[e] Istituto di Biofisica, Consiglio Nazionale delle Ricerche, Via De Marini 6 - Torre di Francia, 16149 Genova, Italy

ARTICLE INFO

Keywords:
Obesity
Adipocyte hypertrophy
Co-culture
Conditioned medium
Hepatocytes dysfunction

ABSTRACT

Hepatic steatosis is often a consequence of obesity. Adipose tissue is an important endocrine regulator of metabolic homeostasis in the body. In obesity, adipocytes become hypertrophic and develop an inflammatory phenotype, altering the panel of secreted adipokines. Moreover, excess fatty acids are, in part, released by adipocytes and delivered to the liver. These multiple pathways of adipose-liver crosstalk contribute to the development and progression of liver disease: TNFα induces hepatocyte dysfunction, excess of circulating fatty acids promotes hepatic steatosis and inflammation, whilst adipokines mediate and exacerbate liver injury. In this study, we investigated *in vitro* the effects and mechanisms of the crosstalk between adipocytes and hepatocytes, as a function of the different adipocyte status (mature *vs* hypertrophic) being mediated by soluble factors. We employed the conditioned medium method to test how mature and hypertrophic adipocytes distinctively affect the liver, leading to metabolic dysfunction. The media collected from adipocytes were characterized by high triglyceride content and led to lipid accumulation and fat-dependent dysfunction in hepatocytes. The present findings seem to suggest that, in addition to triglycerides, other soluble mediators, cytokines, are released by mature and hypertrophic adipocytes and influence the metabolic status of liver cells. Understanding the precise factors involved in the pathogenesis and pathophysiology of NAFLD in obesity will provide important insights into the mechanisms responsible for the metabolic complications of obesity, paving the way for new possible approaches.

1. Introduction

The adipose tissue has the main function of storing energy in the body, following uptake of circulating long-chain fatty acids and intracellular assembly of triglycerides (TGs). However, the white adipose tissue also acts as an endocrine organ secreting a panel of soluble factors, adipokines and hormones which affect other tissues and organs [1]. The adipogenesis process involves progressive TG accumulation in cytosolic lipid droplets leading to differentiation of pre-adipocytes toward a mature adipocyte phenotype. When energy intake exceeds the energy consumption/expenditure, obesity takes place [2]. Obesity consists in an increase in the mass of adipose tissue resulting from adipocyte hypertrophy and/or hyperplasia [3]. In obesity, the hypertrophic adipocytes develop an inflammatory phenotype, secreting inflammatory cytokines into circulation, such as the tumor necrosis factor (TNF)α [4].

The global burden of obesity impacts across multiple organs and diseases, and the main consequence is the metabolic syndrome, a clustering of disorders such as nonalcoholic fatty liver disease (NAFLD), diabetes mellitus, cardiovascular disease, stroke, cancers [5]. NAFLD spectrum ranges from simple steatosis (≥5 % hepatic fat accumulation) to nonalcoholic steatohepatitis (NASH) which may progress toward cirrhosis and hepatocellular carcinoma [6,7]. In molecular terms, steatosis occurs when the rate of hepatic fatty acid uptake from plasma and/or *de novo* fatty acid synthesis is greater than the rate of fatty acid

* Corresponding author at: Dipartimento di Scienze della Terra, dell'Ambiente e della Vita (DISTAV), Corso Europa 26, 16132 Genova, Italy.
E-mail addresses: francesca.baldini@iit.it (F. Baldini), diabfarah2@gmail.com (F. Diab), nadia2296@yahoo.com (N. Serale), lama.zeaiter@iit.it (L. Zeaiter), piero.portincasa@uniba.it (P. Portincasa), alberto.diaspro@iit.it (A. Diaspro), laura.vergani@unige.it (L. Vergani).

https://doi.org/10.1016/j.lfs.2023.121464
Received 7 September 2022; Received in revised form 25 January 2023; Accepted 27 January 2023
Available online 31 January 2023

oxidation and export, thus steatosis representing an imbalance in the complex network of metabolic events [8].

Mounting evidence suggest a strong connection between adipose tissue and liver, being sustained by a complex crosstalk between adipocytes and hepatocytes [9–11]. The panel of soluble factors released by adipocytes should change when they become hypertrophic, and our starting hypothesis is that an *in vitro* approach using cultured adipocytes (mature *vs* hypertrophic) and hepatocytes might unravel pathogenetically relevant mechanisms linking liver and adipose tissue dysfunction. Indeed, is well known that the intercellular communication is mediated not only by direct cell-to-cell interaction, but specifically by secretion of different factors [12]. Among different methods for exploring cell-to-cell crosstalk *in vitro*, the use of conditioned media is often the best way to test for role of soluble factors being involved and, at the same time, to avoid the reciprocal signaling between cells.

In this paper, we investigated *in vitro* the effects of either mature or hypertrophic adipocytes on the multiple physio-pathological responses of cultured hepatocytes. In the experiments, pre adipocytes were firstly differentiated into mature adipocytes, then cultured with long-chain fatty acids to induce hypertrophy and, at the end of the treatment, the conditioned medium from different adipocyte samples was collected and added to the second culture, the hepatocytes.

2. Materials & methods

2.1. Chemicals

All chemicals, unless otherwise indicated, were supplied by Sigma-Aldrich Corp. (Milan, Italy).

2.2. Cell culture and treatments

3T3-L1 mouse fibroblasts were purchased from the American Type Culture Collection (Manassas, VA, USA) and kindly provided by Prof. Bruzzone (University of Genoa). Cells were maintained in Dulbecco's modified Eagle medium (D-MEM) containing 25 mmol/L glucose and 10 % Foetal Bovine Serum (FBS, Euroclone, Milan, Italy) at 37 °C. To induce differentiation, cells were seeded at 2×10^5 cells/mL in multi-well plates. At 2-day post confluence, adipogenesis was induced by adding the differentiation mixture containing 1.7 μM insulin, 1 μM dexamethasone (DEX), and 500 μM 3-isobuthyl-1-methylxanthine (IBMX) for 2 days. Then, cells were incubated with 1.7 μM insulin for 7 days, changing the medium every 2–3 days. Hypertrophy was induced by exposing mature adipocytes to the long-chain fatty acids oleate and palmitate at a final concentration of 0.75 mM (2:1 M ratio), as previously described in detail [13].

FaO cells (European Collection of Authenticated Cell Cultures, Sigma-Aldrich) are a rat hepatoma cell line maintaining hepatocyte-specific markers. Cells were grown in a humidified atmosphere with 5 % CO_2 at 37 °C in Coon's modified Ham's F12 medium supplemented with L-Glutamine and 10 % foetal bovine serum (FBS) [14].

2.3. Co-culture method

To mimic *in vitro* the crosstalk between the adipose tissue and liver tissue in a similar overweight condition, and to focus on potential involvement of soluble mediators, we employed a co-culture technique. 3T3 cells were treated as above described. After treatments, cells were left for 72 h in fresh F12 standard medium thus obtaining the

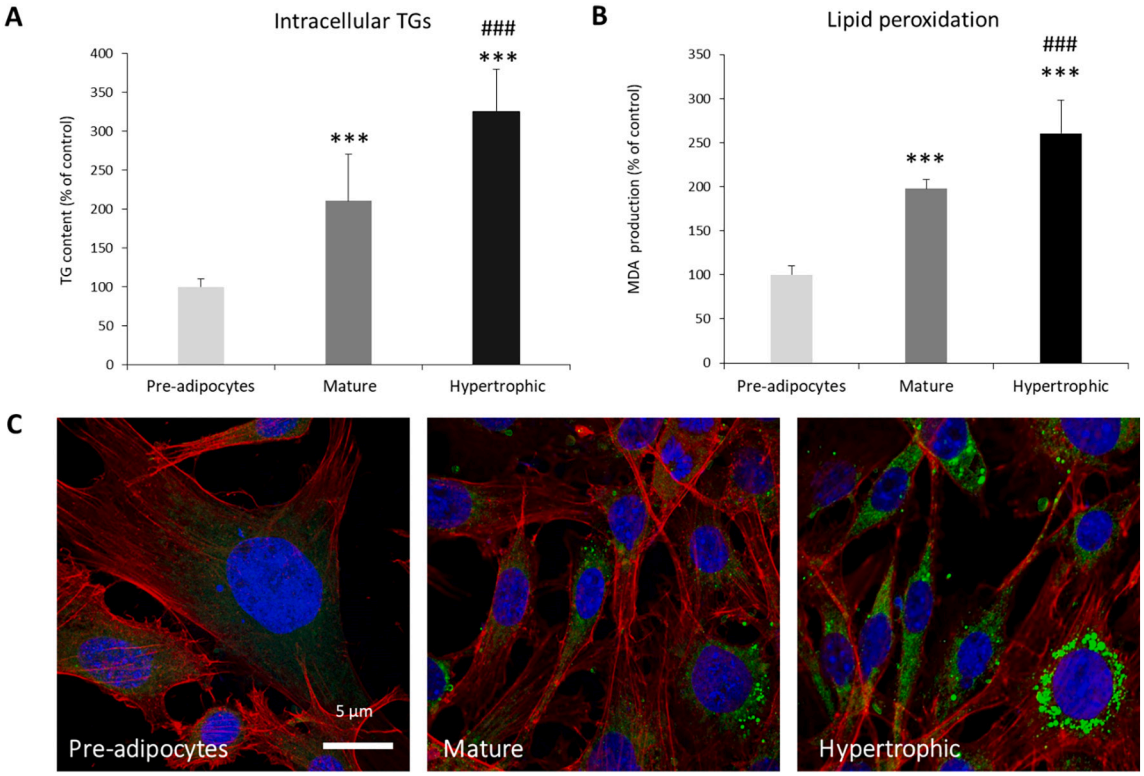

Fig. 1. Lipid accumulation in mature and hypertrophic adipocytes. In 3T3-L1 cells mimicking pre-adipocyte, mature and hypertrophic adipocytes we show: (A) TG content expressed as percent TG content relative to control, normalized for proteins determined with Bradford assay. (B) The intracellular level of MDA (pmol MDA/mL × mg of sample protein) quantified by TBARS assay. Data are expressed as percentage values with respect to controls, normalized for proteins determined with Bradford assay. Values are mean ± S.D. from at least five images from random fields in each treatment. Statistical significance between groups was assessed by ANOVA followed by Tukey's test. Symbols: Ctrl *vs* all treatments ***$p \leq 0.001$; MIX *vs* all treatments ###$p \leq 0.001$. (C) Images of cells (Bar: 5 μm) stained simultaneously with BODIPY 493/503, phalloidin-aberrior STAR 580 and Hoechst 33342. Images were acquired with a Nikon's A1R MP confocal laser scanning microscope, using an Apo TIRF 60 × 60/1.49 oil immersion objective lens (Nikon, Tokyo, Japan), sequentially and then merged.

conditioned medium from adipocyte cells (ACM) (Fig. 1). Different ACMs were then collected, spin to remove cells and debris, and used to treat FaO cells which had grown until 80 % confluence. Cells were incubated as follows: (*i*) fresh unconditioned F12 medium was added to FaO as negative control; (*ii*) ACMs recovered from differently treated 3 T3 cells was added to FaO cells. Then FaO cells were grown for 48 h.

2.4. Protein quantification

The protein content was determined by the Bradford assay using BSA as a standard [15].

2.5. Apoptosis

Cell apoptosis was determined using the FITC-Annexin V Apoptosis Detection Kit (Becton Dickinson Canto II, BD Biosciences, San Jose, CA). After treatments, FaO cells were scraped and stained for 15 min at room temperature in the dark. To discriminate between early and late apoptosis, cells were also stained with 7-amino-actinomycin d (7-AAD). Measurements were performed using a FACS instrument (Becton Dickinson Canto II) and apoptotic fractions were identified and quantified in dot plots using the BD FACSDiva software [16].

2.6. Quantification of triglycerides

Cells were scraped, collected, and lysed. Lipids were extracted in chloroform/methanol (2:1), after evaporation TG content was determined using the 'Triglycerides liquid' kit (Sentinel Diagnostic, Milan, Italy) [17]. Spectrophotometric reading was performed with a Varian Cary-50Bio UV-VIS spectrophotometer (Agilent, Milan, Italy). Values were normalized for the protein content.

2.7. Quantification of intracellular ROS

The oxidation of the cell-permeant 2′-7′ dichlorofluorescin diacetate (DCF-DA, Fluka, Germany) to 2′-7′dichlorofluorescein (DCF) allowed to quantify the production of H_2O_2 and other ROS [18]. Stock solution of DCF-DA (10 mM in DMSO) was prepared and stored at −20 °C in the dark. At the end of treatment, cells were scraped and gently spun down (600 ×*g* for 10 min at 4 °C). After washing, cells were loaded with 10 mM DCF-DA in PBS for 30 min at 37 °C in the dark. Then, cells were centrifuged, suspended in PBS and the fluorescence was measured fluorometrically (λex = 495 nm; λem = 525 nm) [19]. All measurements were performed in a Cary Eclipse Fluorescence Spectrophotometer at 25 °C using a water-thermostated cuvette holder. The fluorescence signal was normalized for the protein content. Values were normalized for the protein content.

2.8. Analysis of lipid peroxidation

Lipid peroxidation was determined through the thiobarbituric acid reactive substances (TBARS) assay which is based on the reaction of malondialdehyde (MDA; 1,1,3,3-tetramethoxypropane) with thiobarbituric acid (TBA) [20]. Briefly, 1 vol. of cell suspension was incubated for 45 min at 95 °C with 2 vol. of TBA solution (0.375 % TBA, 15 % trichloroacetic acid, 0.25 N HCl). Then, 1 vol. of N-butanol was added, and spectrophotometric analyses were carried out at 25 °C recording absorbance at read at 532 nm. The MDA level was expressed as pmol MDA/mL/mg protein [13].

2.9. RNA extraction and real-time qPCR

RNA was isolated using Trizol reagent, cDNA was synthesized, quantitative real-time PCR (qPCR) was performed in quadruplicate using 1× IQ™SybrGreen SuperMix and Chromo4™ System apparatus (Bio-Rad, Milan, Italy) as previously described [13]. The relative quantity of target mRNA was calculated by using the comparative Cq method using the glyceraldehyde 3-phosphate dehydrogenase (GAPDH) as reference gene. The choice of GAPDH gene depends on its central role in the glucose metabolism, and GAPDH was reported to be the optimum gene in mouse models of liver injury [21]. The expression of the target genes was then calculated as relative quantity of mRNA (fold induction) with respect to pre-adipocytes. Primer pairs were designed *ad hoc* starting from the coding sequences of *Rattus norvegicus* and *Mus musculus* (http:// www.ncbi.nlm.nih.gov/Genbank/GenbankSearch.html) and are listed in Table 1.

2.10. Immunofluorescence staining

Cells grown on collagen-coated coverslips were rinsed with phosphate buffered saline (PBS) at pH 7.4 and fixed with 4 % paraformaldehyde in PBS for 15 min. After three times washing in PBS, fixed cells were permeabilized with 0.15 % Triton X-100 and nonspecific binding was blocked with 3 % Albumin from Bovine Serum (BSA) for 1 h at room temperature (RT) [22]. After several washing (3 times for 10 min), slides were incubated at RT for 45 min with 1 μg/mL BODIPY 493/503 (Molecular Probes, Life Technologies, Monza, Italy), to visualize lipid droplets, and phalloidin-aberrior STAR 580 (Aberrior, Göttingen, Germany) to visualize F-actin, in PBS. Then, the cells were incubated with Hoechst 33342 (Invitrogen, Thermo Fisher Scientific, Massachusetts, USA) to detect the nuclear structure. Finally, slides were sealed, and images were acquired with a Nikon's A1R MP confocal laser scanning microscope, using an Apo TIRF 60 × 60/1.49 oil immersion objective lens (Nikon, Tokyo, Japan) and processed by using ImageJ software (https://imagej.net/Fiji/Downloads).

2.11. Oil-Red O staining

Neutral lipids were visualized using the selective Oil-Red O (ORO) dye. Cells grown on collagen-coated coverslips were rinsed PBS and fixed as described above. After fixation, cells were washed with PBS, stained for 20 min with 0.3 % ORO solution prepared from a stock 0.5 % in isopropanol. After washing, slides were examined by Leica DMRB light microscope equipped with a Leica CCD camera DFC420C (Leica, Wetzlar, Germany) using a using a PL FLUOTAR 40×/0.70 PH2 objective lens. Lipid droplets (LDs) analysis was conducted using the free ImageJ software (https://imagej.net/Fiji/Downloads [13]. Briefly, the acquired colour images were converted into 8-bit grayscale images. Then, a threshold was selected to convert the grayscale image to a binary image. Finally, "Analyze Particle" function was used to run the automated analysis. A separate "Results" window provided the area and size of each particle.

2.12. Cytokines analysis

The conditioned medium was collected from adipocytes in different conditions (pre-adipocytes, mature and hypertrophic) after 48 h of incubation. The profiling of the main pro-inflammatory cytokines released into the conditioned media was quantitatively assessed using the mouse obesity enzyme-linked immunosorbent assay (ELISA) Strip I (Signosis, Sunnyvale, CA, USA), according to the manufacturer's instructions. The assay compared the protein expression level of the following eight cytokines: leptin, TNFα, IGF-1, IL-6, VEGF, IL-1α, IL-1β, and MCP-1. Absorbance of each well was measured with a microplate reader Varian Cary-50Bio UV-VIS spectrophotometer (Agilent, Milan, Italy) at 450 nm within 30 min. Values were normalized for the protein content.

2.13. Statistical analysis

Data were expressed as means ± standard deviation (S.D.) of at least three independent experiments in triplicate. Statistical analysis was performed using ANOVA with Tukey's post-hoc test (GraphPad

Table 1
Primer pair sequences. Characteristics of the primer pairs used for the RT-qPCR analysis.

Primer name	Primer sequence 5′- > 3′	Annealing temperature (°C)	Accession ID
GAPDH Fwd	GACCCCTTCATTGACCTCAAC	60	DQ403053
GAPDH Rev	CGCTCCTGGGAAGATGGTGATGGG		
IkBip Fwd	CAGAACAGTGAGCAGGCAAG	60	NM_001009430.2
IkBip Rev	ACGGCATTCTCTATGGTTGG		
PPARα Fwd	CCCCACTTGAAGCAGATGACC	60	NM_013196
PPARα Rev	CCCTAAGTACTGGTAGTCCGC		
Atg7 Fwd	CCTCAGCGGATGTATGGACC	60	NM_001012097.1
Atg7 Rev	AGCCACATTACACCCCAAGG		
UCP2 Fwd	CGTCGGACCTAGCCGTCTGCA	60	NC_013669.1
UCP2 Rev	CGGAGTCGGGAGGGTGCTTTG		
Adiponectin Fwd	GCTCTCCTGTTCCTCTTAATCC	60	NC_000082.6
Adiponectin Rev	GCAATCTCTGCCATCACG		

Software, Inc., San Diego, CA, USA).

3. Results

3.1. Lipid accumulation during maturation and hypertrophy of adipocytes

As a model of adipogenesis *in vitro*, the 3T3-L1 pre-adipocytes were exposed to a differentiating mix to induce maturation into adipocytes, and then they were treated with long chain fatty acids to induce hypertrophy [13]. The lipid accumulation during adipocyte differentiation and hypertrophy was quantified spectrophotometrically showing a progressive significant increase in the intracellular TG content from pre-adipocytes to mature (+110 %, $p \leq 0.001$) and to hypertrophic (+225 %; $p \leq 0.001$) adipocytes (Fig. 1A).

Staining of adipocytes with phalloidin, BODIPY and Hoechst allowed us to selectively label actin filaments, LDs and nuclear DNA, respectively, for confocal microscopy analysis. The representative images of pre-adipocytes, mature and hypertrophic adipocytes (Fig. 1C) attest appreciable morphological changes during the process of *in vitro* adipogenesis and hypertrophy. In particular, the progressive fat accumulation resulted in increased size and number of cytosolic LDs during adipogenesis and even more in hypertrophic cells. Moreover, LDs biogenesis led to modifications of whole cell and nuclear morphology. Indeed, during maturation and hypertrophy adipocytes became more spread on the substrate and these morphometric changes of the cells reflected on the nuclei which became more elongated assuming an ellipsoidal shape and were encircled by numerous lipid droplets.

Lipid accumulation typically results in increased fat oxidation producing excess of ROS which, if not counteracted, may damage different cellular components, such as membranes. In our model we observed an increase in the MDA levels in mature adipocytes with respect to pre-adipocytes (+98 %; $p \leq 0.01$), and an even larger increase (+161 %, $p \leq 0.01$) in hypertrophic cells (Fig. 1B).

Adipogenesis and hypertrophy of adipocytes promote lipid accumulation and oxidative stress in co-cultured hepatocytes.

To mimic the crosstalk between adipose tissue and liver during normal or overweight/obesity conditions, cultured hepatocytes were incubated with the **(**ACM**)** collected from the different stages of adipogenesis/hypertrophy (Fig. 2).

The microscopy analysis showed that treatment with ACM promoted steatosis in hepatocytes in a manner depending on the adipocyte status (Fig. 3A). In detail, co-culture with mature adipocytes promoted large lipid accumulation in FaO cells (about +40 %; $p \leq 0.05$) compared to control cells (namely, FaO cells co-cultured with pre-adipocytes). A more remarkable increase was evident in FaO cells co-cultured with hypertrophic adipocytes (+98 %; $p \leq 0.001$) (Fig. 3B).

Accumulation of cytosolic LDs in FaO cells was visualized and analyzed by ORO staining and optical microscopy (Fig. 4A). Both the number and size of LDs increased in hepatocytes co-cultured with mature adipocytes compared to control (FaO co-culture with pre-adipocytes). In details, in hepatocytes co-cultured with mature adipocytes the LDs average size increased of +43 % ($p \leq 0.05$) compared to control cells, and of +75 % ($p \leq 0.05$) in hepatocytes co-cultured with hypertrophic adipocytes (Fig. 4B). The increase in LDs size was accompanied with an increase in the number of LDs/cell (Fig. 4C). In details, about 361 LDs/100 μm^2 were detected in FaO cells co-cultured with mature adipocytes ($p \leq 0.001$ *vs* pre-adipocyte-ACM) and about 640 LDs/100 μm^2 in FaO cells co-cultured with hypertrophic adipocytes.

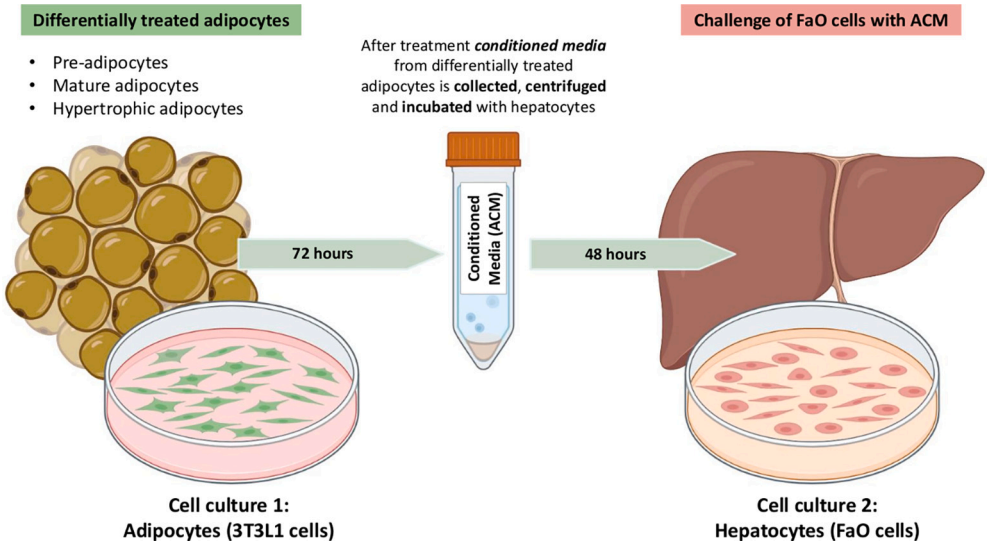

Fig. 2. Representative scheme for co-culture protocol of adipocytes and hepatocytes using conditioned medium. Adipocytes (3T3L1 cells) were firstly differentiated to induce adipogenesis and later incubated with oleate and palmitate to induce hypertrophy. After treatment, adipocytes well left for 72 h to release into the medium differently mediators. Then, the adipocyte conditioned medium (ACM) from pre-adipocytes, mature and hypertrophic adipocytes, was collected, centrifuged, and used to treat cultured FaO cells (~ 80 % confluency) for 48 h. Image created with Biorender.com

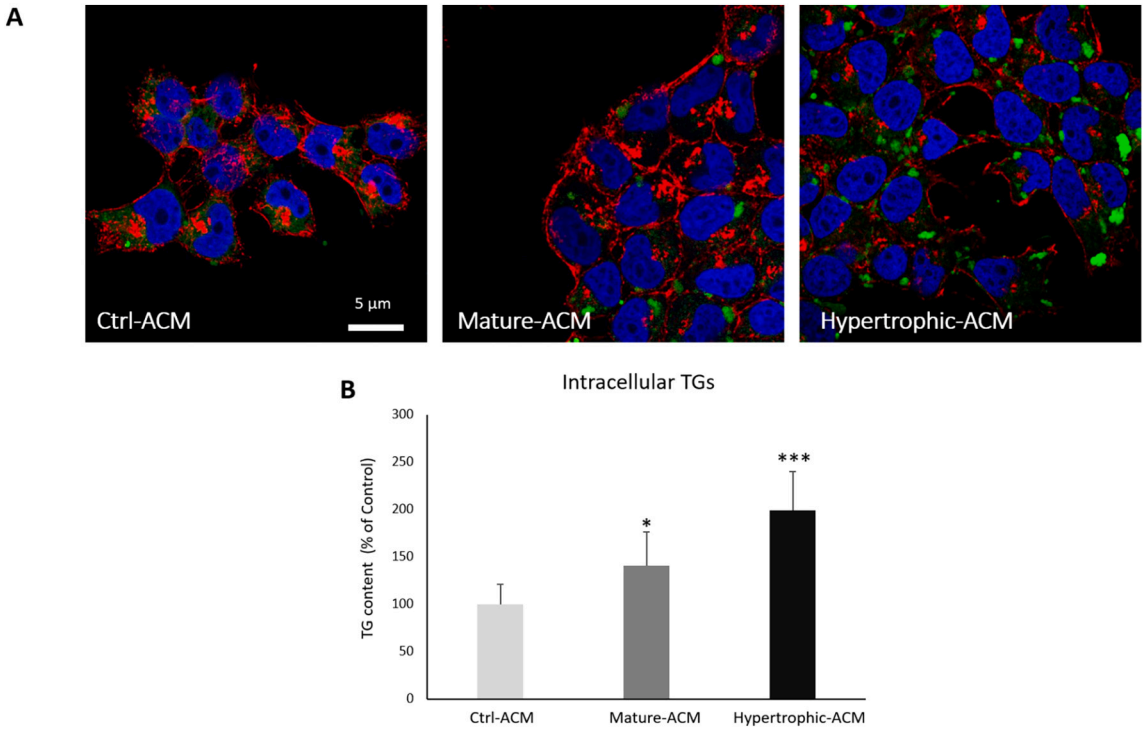

Fig. 3. ACM from differently treated adipocytes trigger different lipid accumulation in hepatocytes. FaO cells were incubated for 72 h with the adipocyte conditioned medium (ACM) collected from pre-adipocytes, mature and hypertrophic adipocytes. (A) Images of cells (Bar: 5 μm) stained simultaneously with BODIPY 493/503, phalloidin-aberrior STAR 580 and Hoechst 33342. Images were acquired as previously described using a Nikon's A1R MP confocal laser scanning microscope, with an Apo TIRF 60 × 60/1.49 oil immersion objective lens (Nikon, Tokyo, Japan). (B) TG content expressed as percent TG content relative to control, normalized for proteins determined with Bradford assay. Values are mean ± S.D. from at least five images from random fields in each treatment. Statistical significance between groups was assessed by ANOVA followed by Tukey's test. Symbols: Ctrl-ACM *vs* all treatments * $p \leq 0.05$, ** $p \leq 0.01$, ***$p \leq 0.001$.

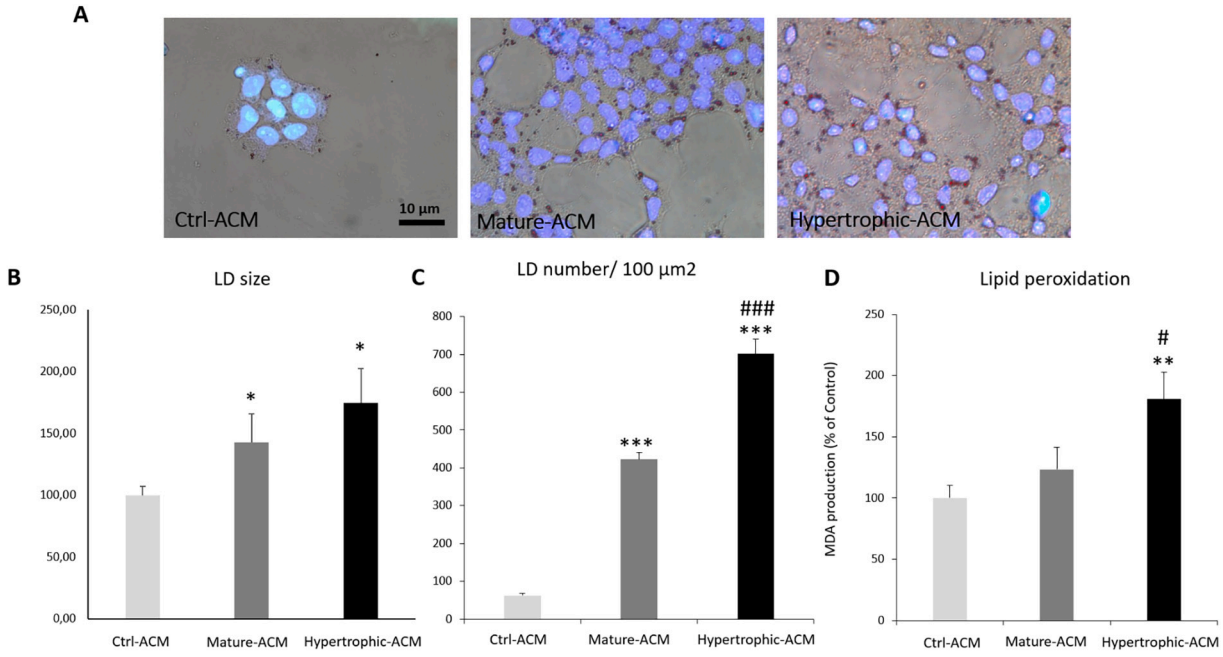

Fig. 4. Adipogenesis and hypertrophy of adipocytes promote lipid accumulation and oxidative stress in hepatic cells. (A) Images of cells stained with Hoechst 33342 and Oil Red-O (ORO) (Bar: 10 μm). Images were acquired sequentially with a Leica DMRB light microscope equipped with a Leica CCD camera DFC420C, using a PL FLUOTAR 40×/0.70 PH2, and then merged. The average size (B) and number (C) of Lipid Droplets calculated using ImageJ free software (http://imagej.nih.gov/ij/). (D) Intracellular MDA level was quantified by TBARS assay as pmol MDA/mL x mg of sample protein.

The enlargement of LDs was statistically significant ($p \leq 0.001$).

In the liver, excess fat accumulation is commonly associated with increased production of oxygen radicals (ROS). We measured the level of membrane lipid peroxidation as a marker of fat-induced ROS production and oxidative stress. As shown in Fig. 4D, FaO cells incubated with ACM from hypertrophic adipocytes showed an increased oxidative stress as indicated by the increase in MDA level (+81 %; $p \leq 0.01$) compared to FaO cells incubated with ACM from mature adipocytes, where the lipid peroxidation did not show significant differences with respect to control FaO cells.

3.2. Adipogenesis and hypertrophy of adipocytes modulate gene expression in co-cultured hepatocytes

The changes in gene transcription profile of hepatocytes co-cultured with adipocytes have been assessed by real time PCR focusing on a panel of genes potentially involved in the liver dysfunction (Fig. 5).

Atg7 is a key gene involved in promoting autophagy, which represents one of the initial mechanisms of protection in the liver during steatosis. The mRNA expression of Atg7 was markedly up-regulated in hepatocytes co-cultured with ACM from mature adipocytes, and furtherly increased by co-culture with ACM from hypertrophic adipocytes compared to control (1.65- and 2.23-fold induction, respectively; $p \leq 0.01$) (Fig. 5A).

PPARα is a nuclear transcription factor involved in the control of lipid metabolism; in particular, it regulates fatty acids uptake, catabolism and turnover. Similarly, PPARα mRNA expression showed a remarkable up-regulation in hepatocytes incubated with both mature-ACM (1.36-fold induction; $p \leq 0.05$ *vs* control) and hypertrophic-ACM (1.41-fold induction; $p \leq 0.05$ *vs* control) adipocytes (Fig. 5B).

IkBip, a serine kinase which plays a role in NF- κB pathway, is a classical marker of liver dysfunction. IkBip mRNA expression increased significantly only in hepatocytes co-cultured with ACM from mature adipocytes (1.46-fold induction; $p \leq 0.05$ *vs* control), but not in hepatocytes co-cultured with ACM from hypertrophic adipocytes (Fig. 5C).

By contrast, UCP2 mRNA expression was up-regulated in hepatocytes exposed to mature adipocytes-ACM (1.59-fold induction; $p \leq 0.05$ *vs* control), but this up-regulation dramatically decreased when hepatocytes were treated with hypertrophic adipocytes-ACM (0.45-fold induction; $p \leq 0.05$ *vs* control) (Fig. 5D). UCP2, a protein involved in uncoupling mitochondrial respiration from ATP synthesis, is known to be involved in various stages of NAFLD progression.

3.3. The panel of soluble factors released by adipocytes changes during adipogenesis and hypertrophy

Adipocyte hypertrophy is often associated with an increase in TG secretion as an attempt to counteract excessive fat accumulation. We observed this increase in mature adipocytes respect to pre-adipocytes (+237 %; $p \leq 0.05$) and even more evident in hypertrophic adipocytes (+237 %; $p \leq 0.05$) (Fig. 6A).

The expression of adiponectin, a classical marker for adipogenesis, was assessed by qPCR. Mature adipocytes showed a significant over-expression of adiponectin mRNA (2341-fold induction *vs* pre-adipocytes; $p \leq 0.001$) compared to pre-adipocytes, without further rise in hypertrophic adipocytes (2542-fold induction *vs* pre-adipocytes; $p \leq 0.001$) (Fig. 6B). This result confirms that reliability of our *in vitro* model of adipogenesis and indicates that we mimicked a condition of early hypertrophy.

The possible changes in the release of eight pro-inflammatory cytokines (leptin, TNFα, IGF-1, IL-6, VEGF, IL-1α, IL-1β, and MCP-1) were assessed by ELISA assay. As shown in Fig. 6C, a general trend to increase was observed for almost all cytokines, some more than others, during *in vitro* differentiation and hypertrophy. In details, going from pre-adipocytes to mature and hypertrophic adipocytes a significant increase was measured in the release of leptin (+90 % and + 87 %; $p \leq 0.01$), VEGF (+97 % and + 104 %; $p \leq 0.001$) and IL-1β (+88 % and +

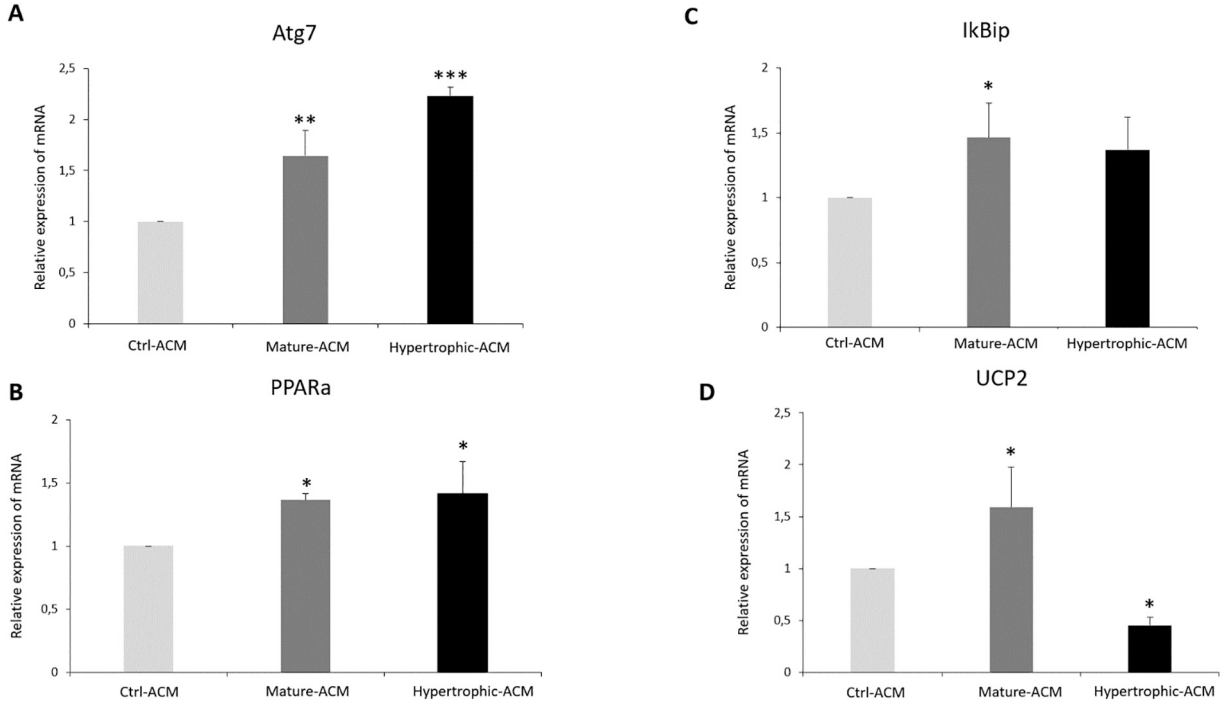

Fig. 5. Adipogenesis and hypertrophy of adipocytes modulate gene expression in hepatic cells. Real-time qPCR analysis of: (A) Atg7; (B) PPARa; (C) IkBip; (D) UCP2 transcriptional expression in FaO cells exposed to different ACMs. The relative quantity of target mRNA was calculated by the comparative Cq method using glyceraldehyde 3-phosphate dehydrogenase (GAPDH) as housekeeping gene and expressed as fold induction with respect to controls. Values are mean ± S.D. from at least three independent experiments. Statistical significance between groups was assessed by ANOVA followed by Tukey's test. Symbols: Ctrl-ACM *vs.* all treatments *$p \leq 0.05$, **$p \leq 0.01$, ***$p \leq 0.001$.

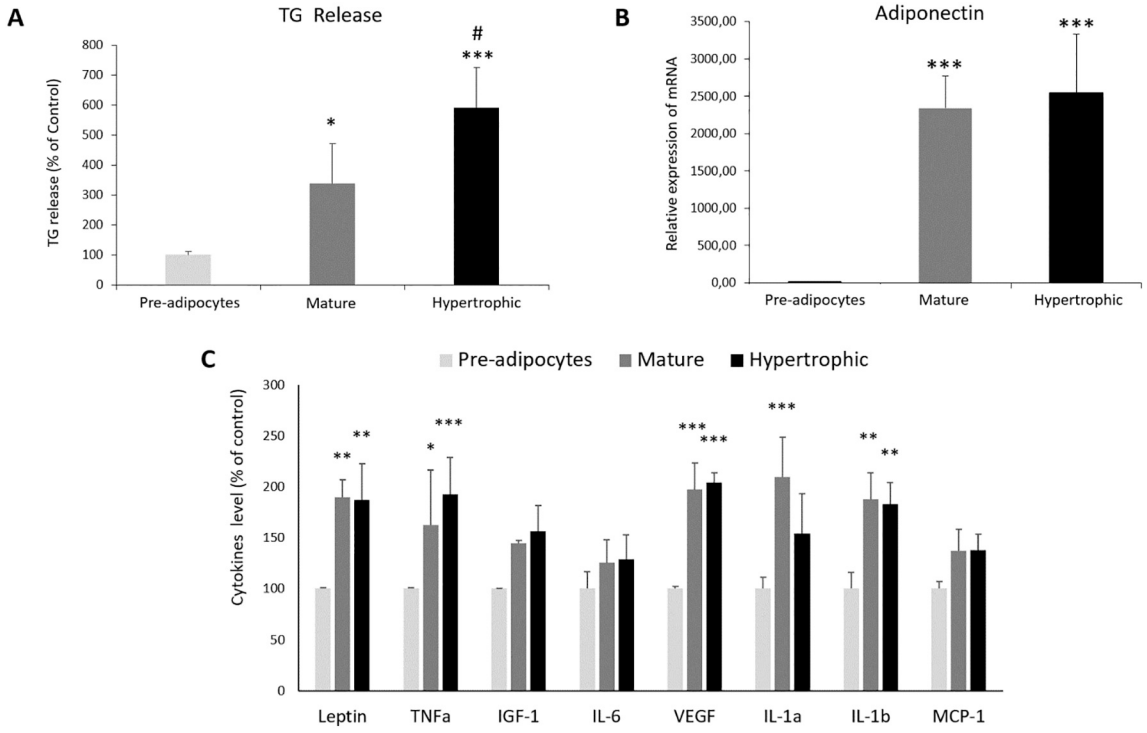

Fig. 6. Soluble factors released by adipocytes changes during adipogenesis and hypertrophy. (A) The extracellular triglyceride (TG) content released into the adipocytes medium. TG content was expressed relative to controls. (B) Real-time qPCR analysis of Adiponectin transcriptional expression in FaO cells exposed to different ACMs. The relative quantity of target mRNA was calculated and expressed as previously described. (C) The level of following soluble cytokines was determined using an enzyme-linked immunosorbent assay: Leptin, TNF alpha, IGF-1, IL-6, VEGF, IL-1 alpha, IL-1 beta, and MCP-1. Results were normalized for proteins content determined with Bradford assay. Values are mean ± S.D. from at least three independent experiments. Statistical significance between groups was assessed by ANOVA followed by Tukey's test. Symbols: Ctrl *vs.* all treatments *p ≤ 0.05, **p ≤ 0.01, ***p ≤ 0.001; MIX *vs.* all treatments #*p* ≤ 0.05.

83 %; $p \leq 0.01$). Notably, the level of TNFα, one of the main inflammatory cytokines, was significantly increased in mature adipocytes (+62 %; $p \leq 0.05$) and even more in hypertrophic adipocytes (+92 %; $p \leq 0.001$). An opposite result was observed for IL-1α that showed a marked release in mature adipocytes (+109 %; $p \leq 0.001$), but the release was reduced by half in hypertrophic cells (+54 %, $p \leq 0.001$). On the other hand, only a slight and no significant increase was observed in the release of IGF-1, IL-6 and MCP-1 during the adipogenic and hypertrophic processes.

4. Discussion

Adipose tissue is the main energy-storing reservoir, but it contributes to other physiological functions such as control of energy homeostasis, food intake, inflammatory response [23]. The close interplay between the adipose tissue and the liver might explain the complex and multiple dysfunctions occurring in obesity [24].

Our *in vitro* model allowed to unveil the mechanisms of crosstalk between adipocytes and hepatocytes, thus improving the understanding of the obesity-dependent liver dysfunction. The main findings of the present study highlighted how the extent of fat accumulation at single adipocytes level may distinctively govern hepatocyte dysfunction at a cellular and molecular level without cell-to-cell interactions.

We adopted an *in vitro* model of crosstalk by incubating hepatocytes with conditioned culture medium collected from adipocytes in different status (mature *vs* hypertrophic). The model of adipogenesis and hypertrophy mimics what happens *in vivo* when pre-adipocytes differentiate in mature adipocytes through accumulation of lipids and rearrangement of cell machinery, and then progress toward an early hypertrophic phenotype in overnutrition condition [13]. Lipid accumulation typically results in increased production of oxidant species that can damage different cellular compartments, as for examples membranes. In our model, we could observe an increase in MDA level, a marker for lipid peroxidation, in mature adipocytes and more in hypertrophic cells.

Paralleling the *in vivo* adipogenesis we observed an increase in the TG content in mature adipocytes and a further increase in hypertrophic adipocytes being accompanied by an increase in average size and number of lipid droplets. Moreover, both differentiation and hypertrophy trigger deep phenotypical rearrangements of adipocytes. Adipose cells spread on the substrate during adipogenesis; a larger spreading occurred when the fat depots enlarged in the hypertrophic cells. Interestingly, changes in nuclear morphometry reflected those occurring in the whole cells, with hypertrophic adipocytes showing nuclei more elongated and with ellipsoidal shape compared to mature adipocytes and pre-adipocytes. Further studies are in progress to decipher how adipocyte maturation and hypertrophy can remodel the nuclear architecture.

When hepatocytes were co-cultured with adipocytes *in vitro* we observed the formation and enlargement of cytosolic LDs to store the lipids released by mature and hypertrophic adipocytes. Indeed, an increase in TG release was observed in mature adipocytes, and even more in hypertrophic cells as a probable attempt to overcome the lipid accumulation occurred during the differentiation and hypertrophy process. We highlighted that a different adipocyte condition (mature *vs* hypertrophic) can determine progressive steatotic features in hepatocytes. The number and size of LDs in hepatocytes reached the maximum in hepatocytes co-cultured with hypertrophic adipocytes. This observation agrees with the fact that hepatocytes start to play adipocyte-like functions when the capacity of adipose tissue to store excess energy is diminished [25].

The excessive accumulation of lipids in the liver is known to result in hepatic dysfunction, which is mediated by oxidative imbalance [26]. Oxidative stress is one of the principal pathogenic mechanisms of liver injury in steatohepatitis and other complications [27]. We found that

lipid peroxidation, a downstream effect of excess fat-dependent ROS production, was significantly increased in hepatocytes co-cultured with hypertrophic adipocytes. This result indicates that hepatocytes suffer of an oxidative imbalance when exposed to soluble signaling released by hypertrophic adipocytes, and this suggests that, also *in vivo*, crosstalk mechanisms without cell-to-cell contact might be responsible of promoting hepatic steatosis, dysfunction and oxidative stress as a response to obesity and adipocyte hypertrophy.

For a deeper understanding, hepatocytes co-cultured with adipocytes were assessed for their transcription profile focusing on a panel of genes implicated in liver metabolism and dysfunction. Autophagy is one of the earliest defense mechanisms against excess fat accumulation [28,29]. Indeed, expression of Atg7, a key autophagy-promoting gene, was progressively up-regulated in hepatocytes co-cultured with adipocytes, thus indicating a stimulation of autophagy. PPARs are a family of nuclear transcription factors acting as main controller of lipid metabolism. PPARα typically regulates the expression of genes involved in fatty acid uptake, catabolism, and turnover [30]. Our findings show that ACM from both mature and hypertrophic adipocytes up-regulated PPARα expression in hepatocytes. It is worth noting that LDs biogenesis represents one of the main defense mechanisms against the excess of free fatty acids in the cell, but if intracellular lipids exceed the cellular capacity, the LDs enlargement may deform the hepatocytes leading to dysfunction and consequent metabolic disorder [31]. In this context, the observed PPARα over-expression may represents an attempt of the cells to keep under control an excessive lipid storage through the stimulation of lipid catabolism [32]. As a marker of liver dysfunction, we assessed IkBip, a serine kinase acting in the NF-κB signaling, which is activated by multiple stimuli such as inflammatory cytokines, DNA damages, and other stressors [33]. IkBip expression showed a trend similar to that of PPARα, as it was up-regulated similarly in hepatocytes co-cultured with both mature and hypertrophic adipocytes. This suggests that the crosstalk with adipocytes in different conditions lead to a similar level of dysfunction in hepatocytes. Obesity is known to affect mitochondria which are the main site for fatty acid degradation; steatotic hepatocytes typically enhance mitochondrial β-oxidation to limit excess lipid accumulation. UCP proteins are located in the mitochondrial inner membrane where they act in uncoupling mitochondrial respiration from ATP synthesis. UCP2 has been found to be involved in various stages of NAFLD progression [34]. Interestingly, we observed an up-regulation of UCP2 expression in hepatocytes co-cultured with mature adipocytes, but a drastic reduction in hepatocytes co-cultured with hypertrophic cells. Such a decrease in UCP2 expression may be a sign of mitochondrial dysfunction leading to oxidative stress and cell death. Taken together, both the increase in lipid peroxidation and the inhibition of UCP2 up-regulation point out an impairment of mitochondrial functionality in hepatocytes in a context of obesity characterized by the hypertrophy of adipocytes.

In our experimental approach, the effects of adipocytes on hepatocytes depend exclusively on soluble factors released by adipocytes. It is known that obesity, and mainly the adipocyte hypertrophy, alters the panel of secreted adipokines [35]. Adiponectin is the main adipokine of adipose tissue which regulates glucose levels, lipid metabolism, and insulin sensitivity [36]. We observed an increased adiponectin expression in both mature and hypertrophic adipocytes without differences between these conditions. Of note, adiponectin seems to display *in vivo* opposite effects depending on the subject conditions. Some evidence shown adiponectin reduction in obesity-related diseases, including insulin resistance, type 2 diabetes and cardiovascular disease. In diabetic patients, adiponectin displays protective effects [37], while in the nondiabetic population it shows an inverse association with the risk for diabetes [38].

Other adipokines sustain the endocrine function of adipose tissue and are relevant to the development of metabolic syndrome, diabetes, and cardiovascular disease associated with impairment of adipogenesis [39]. In our study, both adipogenic and hypertrophic processes stimulate *in vitro* the release of a panel of pro-inflammatory cytokines, but no significant differences could be appreciated between the two conditions, except for TNFα and IL-1α.

TNFα is the main pro-inflammatory cytokine in the body and it was markedly boosted in mature adipocytes and even more in hypertrophic cells. TNFα is a key regulator of adipose tissue mass, and it seems to interfere with metabolism and endocrine functions of adipose tissue [40]. In the liver, TNFα triggers numerous biological responses and multiple signaling pathways involved in inflammation, apoptosis, and proliferation. Moreover, TNFα has been implicated in the progression to hepatocellular carcinoma [41], in the pathogenesis of chronic liver inflammation leading to liver fibrosis by promoting the activation of resident hepatic stellate cells into fibrogenic myofibroblast [42]. On that basis, our findings indicate that TNFα, among all the cytokines evaluated, can represents a crucial "soluble" bridge between different adipocyte conditions occurring during obesity status and liver dysfunction.

An opposite change was observed for the cytokine IL-1α resulting markedly secreted by mature adipocytes but, surprisingly, its release was reduced in hypertrophic cells. IL-1 family is mainly involved in inflammatory pathways, tissue remodeling, and cell adhesion, but the involvement in overweight and obesity is still under debate. *In vivo* studies reported a correlation between IL-1α levels and body fat mass [43]. On the other hand, IL-1α seems to impair the adipogenesis through inhibition of PPAR-γ and lipogenic pathways [44]. At hepatic level, different studies highlighted the role of this interleukin in both the early fibrogenesis and the maintenance of fibrosis. In particular, IL-1α is involved in the progression from liver injury to fibrosis [45]. Our finding of a reduction in IL-1α release by hypertrophic adipocytes may suggest that the decrease of this adipokine is a consequence of cell impairment and dysfunction due to the hypertrophy.

In conclusion, our *in vitro* model of adipocyte-hepatocyte crosstalk can mirror the events occurring *in vivo*. This is of interest since this model is a simplified system to dissect complex molecular events that are difficult to investigate *in vivo*. Our findings suggest that both mature and hypertrophic adipocytes modulate hepatocyte functions in terms of LDs biogenesis and accumulation, ROS production and oxidative stress, fatty acid catabolism and mitochondrial impairment. At a molecular level, the conditioned medium from differently treated adipocytes can affect the functionality of hepatic cells through changes in the panel of soluble factors released. Among these factors, the main role seems played by secretion of triglycerides, TNFα and adiponectin from mature and hypertrophic adipocytes. Therefore, the extent of fat accumulation in the adipocytes distinctively triggers liver dysfunction. However, further studies are needed to depict the exact cascade of mechanisms involved to outline potential directions for further research.

CRediT authorship contribution statement

Francesca Baldini: Conceptualization, Data curation, Writing- Original draft preparation; Farah Diab: Data curation, Investigation, Writing- Original draft preparation; Nadia Serale: Data curation, Investigation; Lama Zeaiter: Data curation, Investigation; Piero Portincasa: Conceptualization, Writing- Reviewing and Editing; Alberto Diaspro: Conceptualization, Writing- Reviewing and Editin; Laura Vergani: Conceptualization, Data curation, Writing- Original draft preparation, Supervision.

Funding

This work was supported by grants from University of Genova (FRA 2020).

Data availability

Data will be made available on request.

Acknowledgements

The authors would like to thank Dr. Isotta Cainero (Nanoscopy, IIT, Genova, Italy), Dr. Michele Oneto (Nikon Imaging Center, IIT, Genova, Italy) and Francesca Storace (DISTAV, Genova, Italy) for their experimental assistance.

References

[1] S. Galic, J.S. Oakhill, G.R. Steinberg, Adipose tissue as an endocrine organ, Mol. Cell. Endocrinol. 316 (2010) 129–139, https://doi.org/10.1016/j.mce.2009.08.018.
[2] J.O. Hill, H.R. Wyatt, J.C. Peters, Energy balance and obesity, Circulation 126 (2012) 126–132, https://doi.org/10.1161/CIRCULATIONAHA.111.087213.
[3] A.L. Ghaben, P.E. Scherer, Adipogenesis and metabolic health, Nat. Rev. Mol. Cell Biol. 20 (2019) 242–258, https://doi.org/10.1038/s41580-018-0093-z.
[4] R. Parker, The role of adipose tissue in fatty liver diseases, Liver Res. 2 (2018) 35–42, https://doi.org/10.1016/j.livres.2018.02.002.
[5] T. Kawai, M.V. Autieri, R. Scalia, Adipose tissue inflammation and metabolic dysfunction in obesity, Am. J. Physiol. Physiol. 320 (2021) C375–C391, https://doi.org/10.1152/ajpcell.00379.2020.
[6] E.M. Brunt, V.W.S. Wong, V. Nobili, C.P. Day, S. Sookoian, J.J. Maher, E. Bugianesi, C.B. Sirlin, B.A. Neuschwander-Tetri, M.E. Rinella, Nonalcoholic fatty liver disease, Nat. Rev. Dis. Primers. 1 (2015) 15080, https://doi.org/10.1038/nrdp.2015.80.
[7] M.S. Siddiqui, S.A. Harrison, M.F. Abdelmalek, Q.M. Anstee, P. Bedossa, L. Castera, L. Dimick-Santos, S.L. Friedman, K. Greene, D.E. Kleiner, S. Megnien, B. A. Neuschwander-Tetri, V. Ratziu, E. Schabel, V. Miller, A.J. Sanyal, Case definitions for inclusion and analysis of endpoints in clinical trials for nonalcoholic steatohepatitis through the lens of regulatory science, Hepatology 67 (2018) 2001–2012, https://doi.org/10.1002/hep.29607.
[8] V. Zámbó, L. Simon-Szabó, P. Szelényi, É. Kereszturi, G. Bánhegyi, M. Csala, Lipotoxicity in the liver, World J. Hepatol. 5 (2013) 550, https://doi.org/10.4254/wjh.v5.i10.550.
[9] A. Fougerat, G. Schoiswohl, A. Polizzi, M. Régnier, C. Wagner, S. Smati, T. Fougeray, Y. Lippi, F. Lasserre, I. Raho, V. Melin, B. Tramunt, R. Métivier, C. Sommer, F. Benhamed, C. Alkhoury, F. Greulich, C. Jouffe, A. Emile, M. Schupp, P. Gourdy, P. Dubot, T. Levade, D. Meynard, S. Ellero-Simatos, L. Gamet-Payrastre, G. Panasyuk, H. Uhlenhaut, E.-Z. Amri, C. Cruciani-Guglielmacci, C. Postic, W. Wahli, N. Loiseau, A. Montagner, D. Langin, A. Lass, H. Guillou, ATGL-dependent white adipose tissue lipolysis controls hepatocyte PPARα activity, Cell Rep. 39 (2022), 110910, https://doi.org/10.1016/j.celrep.2022.110910.
[10] O. Kucukoglu, J.-P. Sowa, G.D. Mazzolini, W.-K. Syn, A. Canbay, Hepatokines and adipokines in NASH-related hepatocellular carcinoma, J. Hepatol. 74 (2021) 442–457, https://doi.org/10.1016/j.jhep.2020.10.030.
[11] N. Sahini, J. Borlak, Recent insights into the molecular pathophysiology of lipid droplet formation in hepatocytes, Prog. Lipid Res. 54 (2014) 86–112, https://doi.org/10.1016/j.plipres.2014.02.002.
[12] W.L. Holland, J.Y. Xia, J.A. Johnson, K. Sun, M.J. Pearson, A.X. Sharma, E. Quittner-Strom, T.S. Tippetts, R. Gordillo, P.E. Scherer, Inducible overexpression of adiponectin receptors highlight the roles of adiponectin-induced ceramidase signaling in lipid and glucose homeostasis, Mol. Metab. 6 (2017) 267–275, https://doi.org/10.1016/j.molmet.2017.01.002.
[13] F. Baldini, R. Fabbri, C. Eberhagen, A. Voci, P. Portincasa, H. Zischka, L. Vergani, Adipocyte hypertrophy parallels alterations of mitochondrial status in a cell model for adipose tissue dysfunction in obesity, Life Sci. 265 (2021), 118812, https://doi.org/10.1016/j.lfs.2020.118812.
[14] G. Vecchione, E. Grasselli, F. Cioffi, F. Baldini, P.J. Oliveira, V.A. Sardão, K. Cortese, A. Lanni, A. Voci, P. Portincasa, L. Vergani, The nutraceutic silybin counteracts excess lipid accumulation and ongoing oxidative stress in an in vitro model of non-alcoholic fatty liver disease progression, Front. Nutr. 4 (2017), https://doi.org/10.3389/fnut.2017.00042.
[15] M.M. Bradford, A rapid and sensitive method for the quantitation of microgram quantities of protein utilizing the principle of protein-dye binding, Anal. Biochem. 72 (1976) 248–254, https://doi.org/10.1016/0003-2697(76)90527-3.
[16] F. Baldini, M. Khalil, N. Serale, A. Voci, P. Portincasa, L. Vergani, Extent and features of liver steatosis in vitro pave the way to endothelial dysfunction without physical cell-to-cell contact, Nutr. Metab. Cardiovasc. Dis. 31 (2021) 3522–3532, https://doi.org/10.1016/j.numecd.2021.08.032.
[17] E. Grasselli, A. Voci, L. Canesi, F. Goglia, S. Ravera, I. Panfoli, G. Gallo, L. Vergani, Non-receptor-mediated actions are responsible for the lipid-lowering effects of iodothyronines in FaO rat hepatoma cells, J. Endocrinol. 210 (2011) 59–69, https://doi.org/10.1530/JOE-11-0074.
[18] B. Halliwell, M. Whiteman, Measuring reactive species and oxidative damage in vivo and in cell culture: how should you do it and what do the results mean? Br. J. Pharmacol. 142 (2004) 231–255, https://doi.org/10.1038/sj.bjp.0705776.
[19] M. Khalil, N. Serale, F. Diab, F. Baldini, P. Portincasa, G. Lupidi, L. Vergani, Beneficial effects of carvacrol on in vitro models of metabolically-associated liver steatosis and endothelial dysfunction: a role for fatty acids in interfering with carvacrol binding to serum albumin, Curr. Med. Chem. 29 (2022) 5113–5129, https://doi.org/10.2174/0929867329666220401103643.
[20] H. Iguchi, S. Kojo, M. Ikeda, Lipid peroxidation and disintegration of the cell membrane structure in cultures of rat lung fibroblasts treated with asbestos, J. Appl. Toxicol. 13 (1993) 269–275, https://doi.org/10.1002/jat.2550130409.
[21] S. Wang, J. Wang, X. Lv, Selection of reference genes for expression analysis in mouse models of acute alcoholic liver injury, Int. J. Mol. Med. 41 (2018) 3527–3536, https://doi.org/10.3892/ijmm.2018.3527.
[22] F. Baldini, P. Portincasa, E. Grasselli, G. Damonte, A. Salis, M. Bonomo, M. Florio, N. Serale, A. Voci, P. Gena, L. Vergani, G. Calamita, Aquaporin-9 is involved in the lipid-lowering activity of the nutraceutical silybin on hepatocytes through modulation of autophagy and lipid droplets composition, Biochim. Biophys. Acta - Mol. Cell Biol. Lipids. 1865 (2020), 158586, https://doi.org/10.1016/j.bbalip.2019.158586.
[23] K. Sarjeant, J.M. Stephens, Adipogenesis, Cold Spring Harb. Perspect. Biol. 4 (2012), https://doi.org/10.1101/cshperspect.a008417 a008417-a008417.
[24] Y. Zhao, M.-F. Zhao, S. Jiang, J. Wu, J. Liu, X.-W. Yuan, D. Shen, J.-Z. Zhang, N. Zhou, J. He, L. Fang, X.-T. Sun, B. Xue, C.-J. Li, Liver governs adipose remodelling via extracellular vesicles in response to lipid overload, Nat. Commun. 11 (2020) 719, https://doi.org/10.1038/s41467-020-14450-6.
[25] S.A. Polyzos, C.S. Mantzoros, Leptin in health and disease: facts and expectations at its twentieth anniversary, Metabolism 64 (2015) 5–12, https://doi.org/10.1016/j.metabol.2014.10.017.
[26] Y. Zhong, Y. Pan, L. Liu, H. Li, Y. Li, J. Jiang, J. Xiang, J. Zhang, W. Chu, Effects of high fat diet on lipid accumulation, oxidative stress and autophagy in the liver of chinese softshell turtle (Pelodiscus sinensis), Comp. Biochem. Physiol. Part B Biochem. Mol. Biol. 240 (2020), 110331, https://doi.org/10.1016/j.cbpb.2019.110331.
[27] V.W.-S. Wong, L.A. Adams, V. de Lédinghen, G.L.-H. Wong, S. Sookoian, Noninvasive biomarkers in NAFLD and NASH — current progress and future promise, Nat. Rev. Gastroenterol. Hepatol. 15 (2018) 461–478, https://doi.org/10.1038/s41575-018-0014-9.
[28] S. Kaushik, A.M. Cuervo, Degradation of lipid droplet-associated proteins by chaperone-mediated autophagy facilitates lipolysis, Nat. Cell Biol. 17 (2015) 759–770, https://doi.org/10.1038/ncb3166.
[29] N. Martinez-Lopez, R. Singh, Autophagy and lipid droplets in the liver, Annu. Rev. Nutr. 35 (2015) 215–237, https://doi.org/10.1146/annurev-nutr-071813-105336.
[30] M. Pawlak, P. Lefebvre, B. Staels, Molecular mechanism of PPARα action and its impact on lipid metabolism, inflammation and fibrosis in non-alcoholic fatty liver disease, J. Hepatol. 62 (2015) 720–733, https://doi.org/10.1016/j.jhep.2014.10.039.
[31] F. Baldini, M. Khalil, A. Bartolozzi, M. Vassalli, A.Di Ciaula, P. Portincasa, L. Vergani, Relationship between liver stiffness and steatosis in obesity conditions: in vivo and in vitro studies, Biomolecules 12 (2022) 733, https://doi.org/10.3390/biom12050733.
[32] K.H.H. Liss, B.N. Finck, PPARs and nonalcoholic fatty liver disease, Biochimie 136 (2017) 65–74, https://doi.org/10.1016/j.biochi.2016.11.009.
[33] M. Cnop, F. Foufelle, L.A. Velloso, Endoplasmic reticulum stress, obesity and diabetes, Trends Mol. Med. 18 (2012) 59–68, https://doi.org/10.1016/j.molmed.2011.07.010.
[34] György Baffy, Uncoupling protein-2 and non-alcoholic fatty liver disease, Front. Biosci. 10 (2005) 2082, https://doi.org/10.2741/1683.
[35] X. Unamuno, J. Gómez-Ambrosi, A. Rodríguez, S. Becerril, G. Frühbeck, V. Catalán, Adipokine dysregulation and adipose tissue inflammation in human obesity, Eur. J. Clin. Investig. 48 (2018), e12997, https://doi.org/10.1111/eci.12997.
[36] H. Fang, R.L. Judd, Adiponectin regulation and function, Compr. Physiol. 8 (2018) 1031–1063, https://doi.org/10.1002/cphy.c170046.
[37] C.S. Mantzoros, T. Li, J.E. Manson, J.B. Meigs, F.B. Hu, Circulating adiponectin levels are associated with better glycemic control, more favorable lipid profile, and reduced inflammation in women with type 2 diabetes, J. Clin. Endocrinol. Metab. 90 (2005) 4542–4548, https://doi.org/10.1210/jc.2005-0372.
[38] S. Li, H.J. Shin, E.L. Ding, R.M. van Dam, Adiponectin levels and risk of type 2 diabetes, JAMA 302 (2009) 179, https://doi.org/10.1001/jama.2009.976.
[39] L. Al-Mansoori, H. Al-Jaber, M.S. Prince, M.A. Elrayess, Role of inflammatory cytokines, growth factors and adipokines in adipogenesis and insulin resistance, Inflammation 45 (2022) 31–44, https://doi.org/10.1007/s10753-021-01559-z.
[40] W.P. Cawthorn, J.K. Sethi, TNF-α and adipocyte biology, FEBS Lett. 582 (2008) 117–131, https://doi.org/10.1016/j.febslet.2007.11.051.
[41] Z.-T. Jing, W. Liu, C.-R. Xue, S.-X. Wu, W.-N. Chen, X.-J. Lin, X. Lin, AKT activator SC79 protects hepatocytes from TNF-α-mediated apoptosis and alleviates d-Gal/LPS-induced liver injury, Am. J. Physiol. Liver Physiol. 316 (2019) G387–G396, https://doi.org/10.1152/ajpgi.00350.2018.
[42] Y.M. Yang, E. Seki, TNFα in liver fibrosis, Curr. Pathobiol. Rep. 3 (2015) 253–261, https://doi.org/10.1007/s40139-015-0093-z.
[43] J.-Y. Um, H.-K. Rim, S.-J. Kim, H.-L. Kim, S.-H. Hong, Functional polymorphism of IL-1 alpha and its potential role in obesity in humans and mice, PLoS One 6 (2011), e29524, https://doi.org/10.1371/journal.pone.0029524.
[44] X. Sun, T. Zou, C. Zuo, M. Zhang, B. Shi, Z. Jiang, H. Cui, X. Liao, X. Li, Y. Tang, Y. Liu, X. Liu, IL-1α inhibits proliferation and adipogenic differentiation of human adipose-derived mesenchymal stem cells through NF-κB- and ERK1/2-mediated proinflammatory cytokines, Cell Biol. Int. 42 (2018) 794–803, https://doi.org/10.1002/cbin.10932.
[45] R.G. Gieling, K. Wallace, Y.-P. Han, Interleukin-1 participates in the progression from liver injury to fibrosis, Am. J. Physiol. Liver Physiol. 296 (2009) G1324–G1331, https://doi.org/10.1152/ajpgi.90564.2008.